

THIS REPORT HAS BEEN DELIMITED
AND CLEARED FOR PUBLIC RELEASE
UNDER DOD DIRECTIVE 5200.20 AND
NO RESTRICTIONS ARE IMPOSED UPON
ITS USE AND DISCLOSURE.

DISTRIBUTION STATEMENT A

APPROVED FOR PUBLIC RELEASE;
DISTRIBUTION UNLIMITED.

Armed Services Technical Information Agency

AD

32269

NOTICE: WHEN GOVERNMENT OR OTHER DRAWINGS, SPECIFICATIONS OR OTHER DATA ARE USED FOR ANY PURPOSE OTHER THAN IN CONNECTION WITH A DEFINITELY RELATED GOVERNMENT PROCUREMENT OPERATION, THE U. S. GOVERNMENT THEREBY INCURS NO RESPONSIBILITY, NOR ANY OBLIGATION WHATSOEVER; AND THE FACT THAT THE GOVERNMENT MAY HAVE FORMULATED, FURNISHED, OR IN ANY WAY SUPPLIED THE SAID DRAWINGS, SPECIFICATIONS, OR OTHER DATA IS NOT TO BE REGARDED BY IMPLICATION OR OTHERWISE AS IN ANY MANNER LICENSING THE HOLDER OR ANY OTHER PERSON OR CORPORATION, OR CONVEYING ANY RIGHTS OR PERMISSION TO MANUFACTURE, USE OR SELL ANY PATENTED INVENTION THAT MAY IN ANY WAY BE RELATED THERETO.

Reproduced by
DOCUMENT SERVICE CENTER
KNOTT BUILDING, DAYTON, 2, OHIO

UNCLASSIFIED

AD NC 44-249
ASTIA FILE COPY

Technical Report
to the
Office of Naval Research
Project NR-051-258

ANODIC OXIDATION OF METALS AT
CONTROLLED POTENTIAL

by

P. Detsky, J. Q. Juliano, J. A. Perry, and
G. L. Stinch

Report No. 12

Technical Report
to the
Office of Naval Research

Report No 12
Project NR-051-258

ANODIC OXIDATION OF METALS AT CONTROLLED POTENTIAL -
EXPERIMENTAL METHODS AND CASE OF IRON

by

Paul Delahay, José O. Julianó, John A. Perry, and George L. Stiehl

March 1954
Department of Chemistry
Louisiana State University
Baton Rouge 3, Louisiana

DISTRIBUTION LIST FOR TECHNICAL REPORTS

<u>No. of Copies</u>	<u>Addressee</u>
1	Commanding Officer Office of Naval Research Branch Office 150 Causeway Street Boston, Massachusetts
2	Commanding Officer Office of Naval Research Branch Office The John Crerar Library Building 86 E. Randolph Street Tenth Floor Chicago 1, Illinois
1	Commanding Officer Office of Naval Research Branch Office 346 Broadway New York 13, New York
1	Commanding Officer Office of Naval Research Branch Office 1000 Geary Street San Francisco 9, California
1	Commanding Officer Office of Naval Research Branch Office 1030 N. Green Street Pasadena 1, California
2	Officer-in-Charge Office of Naval Research Branch Office Navy Number 100 Fleet Post Office New York, New York
6	Director, Naval Research Laboratory Washington 25, D. C. Attention: Technical Information Officer
2	Chief of Naval Research Office of Naval Research Washington 25, D. C. Attention: Chemistry Branch
5	ASTIA Document Service Center Knott Building Dayton 2, Ohio
1	Dr. Ralph G. H. Siu, Research Director General Laboratories, QM Dept 2800 S. 20th Street Philadelphia 45, Pennsylvania

DISTRIBUTION LIST FOR TECHNICAL REPORTS

Page 11

No. of CopiesAddressee

1	Dr. Warren Stubblebine, Research Director Chemical and Plastics Section, RDB-MPD Quartermaster General's Office Washington 25, D. C.
1	Dr. A. Stuart Hunter, Tech. Director Research and Development Branch MPD Quartermaster General's Office Washington 25, D. C.
1	Office of Technical Services Department of Commerce Washington 25, D. C.
1	Dr. A. Weiseler Department of the Army Office of the Chief of Ordnance Washington 25, D. C. Attn: ORCTB-PS
1	Research and Development Group Logistics Division, General Staff Department of the Army Washington 25, D. C. Attn: Dr. W. T. Read, Scientific Adviser
2	Director, Naval Research Laboratory Washington 25, D. C. Attention: Chemistry Division
2	Chief of the Bureau of Ships Navy Department Washington 25, D. C. Attention: Code 340
2	Chief of the Bureau of Aeronautics Navy Department Washington 25, D. C. Attention: Code TD-4
2	Chief of the Bureau of Ordnance Navy Department Washington 25, D. C. Attention: Code Rexd
1	Office of the Secretary of Defense Pentagon Room 3D1041 Washington 25, D. C. Attention: Library Branch (R+D)
1	Dr. A. G. Horney Office Scientific Research R and D Command USAF Box 1395 Baltimore, Maryland

DISTRIBUTION LIST FOR TECHNICAL REPORTS

Page III

No. of CopiesAddressee

1	Dr. H. A. Zahl, Tech. Director Signal Corps Engineering Laboratories Fort Monmouth, New Jersey
1	U. S. Naval Radiological Defense Laboratory San Francisco 24, California Attention: Technical Library
1	Naval Ordnance Test Station (Inyokern) China Lake, California Attention: Head, Chemistry Division
1	Office of Ordnance Research 2127 Myrtle Drive Durham, North Carolina
1	Technical Command Chemical Corps Chemical Center, Maryland
1	U. S. Atomic Energy Commission Research Division Washington 25, D. C.
1	U. S. Atomic Energy Commission Chemistry Division Brookhaven National Laboratory Upton, New York
1	U. S. Atomic Energy Commission Library Branch, Tech. Information ORE P. O. Box E Oak Ridge, Tennessee
1	Dr. A. E. Remick Department of Chemistry Wayne University Detroit 1, Michigan
1	Dr. Frank Novorka Department of Chemistry Western Reserve University Cleveland 6, Ohio
1	Dr. David C. Grahame Department of Chemistry Amherst College Amherst, Massachusetts

DISTRIBUTION LIST FOR TECHNICAL REPORTS

Page IV

<u>No. of Copies</u>	<u>Addressee</u>
1	Dr. P. J. Elving Department of Chemistry University of Michigan Ann Arbor, Michigan
1	Dr. N. H. Furman Department of Chemistry Princeton University Princeton, New Jersey
1	Dr. I. M. Kolthoff Department of Chemistry University of Minnesota Minneapolis 14, Minnesota
1	Dr. H. A. Laitinen Department of Chemistry University of Illinois Urbana, Illinois
1	Dr. Louis Meites Department of Chemistry Yale University New Haven, Connecticut
1	Dr. O. H. Muller Department of Physiology Syracuse University Syracuse, New York
1	Dr. Pierre Van Rysselberghe Department of Chemistry University of Oregon Eugene, Oregon
1	Dr. Stanley Wawzonek Department of Chemistry State University of Iowa Iowa City, Iowa
1	Dr. J. J. Lingane Department of Chemistry Harvard University Cambridge 38, Massachusetts
1	Dr. Leon O. Morgan Department of Chemistry University of Texas Austin, Texas

ABSTRACT

Rates of anodic oxidation of iron are measured at constant potential in diluted perchloric acid, acetate and borate buffers, and sodium hydroxide solutions. A treatment for the kinetics of anodic oxidation of metals at constant potential is presented for processes in which a soluble species is formed and processes yielding insoluble products are also interpreted. Experimental methods are described.

The kinetics of the anodic oxidation of metals is involved especially when insoluble products are formed. These processes do not lend themselves to mathematical analysis, and an essentially experimental approach must be followed. Such an approach is adopted here, and results are reported for iron.

EXPERIMENTAL

POTENTIOSTAT.

The potentiostat was a modified version of the instrument described by Lamphere and Rogers¹. So many potentiostats have been described in

(1) R. W. Lamphere and L. B. Rogers, Anal. Chem., **22**, 463 (1950).

the literature² that there is no need for a detailed description here;

(2) J. J. Lingane, "Electroanalytical Chemistry", Interscience, New York, N. Y., 1953, pp. 202-244.

The diagram of Fig. 1 is sufficiently explicit. The potentiostat had an output voltage of approximately 160 volts; the maximum current was 2.4 amperes.

ELECTROLYTIC CELL.

The cell was designed to achieve uniform current density over the whole area of the electrode. The arrangement is quite apparent from Fig. 2. The electrode of the metal being studied was a disk placed at the bottom of the Lucite cell. A disk was pressed against the electrode by means of three screws. Connection (E_1) was obtained by pressing a metallic point on one face of the electrode. A thin (0.2 mm or so) plastic washer inserted between the metal and the wall of the cell ensured tightness. The diameter of the working circular area of the electrode was 2.5 cm. The auxiliary electrode was a platinum disk (E_2) whose diameter was only slightly smaller than that of the effective circular area of the electrode. Electrode E_2 was inserted in a separate compartment whose bottom was a fritted glass disk. An agar-agar plug (not represented in Fig. 2) covered this disk and decreased the rate of diffusion of electrolyte from one compartment to the other. The assembly of electrode E_2 was held by a rubber ring R.

Uniform stirring was obtained by circulating the electrolyte at the rate of 200 ml. min.⁻¹ by means of a pump P (Fig. 2 right) made of uncorrodable material³. Oxygen was removed by bubbling nitrogen in cell C_2 . This cell was maintained at $35 \pm 0.1^\circ$. The total volume of solution was 420 ml.

5

(3) Vanton Corporation, New York, N. Y.

The potential of the working electrode (E_1) was measured against a saturated calomel electrode which was connected to the main cell by a salt bridge (filled with the same electrolyte as the main cell). The usual Haber-Luggin tip for reference electrodes was not utilized, because the resulting shielding of the working electrode causes a local decrease in current density in the area of the electrode where the potential is being measured. This effect was studied extensively by Piontelli and coworkers⁴,

(4) R. Aletti, U. Bertocci, G. Bianchi, C. Guerri, R. Piontelli, G. Poli, and G. Serravalle, Int. Comm. Electrochem. Therm. Kin., Proceedings of 3rd Meeting, Manfredi, Milan, 1953, pp. 30-42.

who recommended a cylindric tip pressed against the electrode. This procedure was used in this study. The end of the tip was made of a Lucite piece which was cemented to an ordinary glass tube. There was virtually no electrolysis at the point of contact, but the current density was otherwise uniform. Connection between electrodes E_1 and E_2 was provided by a small canal 0 (diameter 0.5 mm) whose lower end was in the immediate vicinity of the surface of the working electrode.

TREATMENT OF WORKING ELECTRODE.

The working electrode was made of "pure" iron⁵. The metal was first

(5) Obtained from D. H. Mackay, 198 Broadway, New York, N. Y. The emission spectrum indicated that the metal was at least as pure as "spectroscopically pure iron".

cleaned with acetone and water. It was then immersed for 15-30 sec. in 6 M hydrochloric acid and rinsed with distilled water. The electrode was dried and finally weighed. At the end of electrolysis the electrode was rapidly removed from the cell by unfastening the three screws at the bottom of the cell, the electrolysis circuit remaining closed. The electrode was washed in 6 N. HCl for 30 sec. to remove the products of anodic oxidation; this was followed by washing in water and drying under vacuum. Losses of weight as low as $0.2 - 0.3 \text{ mg. cm.}^{-2} \text{ hr.}^{-1}$ could be measured.

DESCRIPTION AND DISCUSSION OF RESULTS

OXIDATION IN 0.1 N PERCHLORIC ACID.

Rates of oxidation of iron in 0.1 M perchloric acid are plotted against potential in Fig. 3. The rate of oxidation decreases as the potential becomes more cathodic. These results can be explained as follows.

The current for the anodic oxidation of a metal with the formation of a soluble species is

$$i = n F A \left[k_a - k_c f_{M^{+n}} (C_{M^{+n}})_{\infty} \right] \quad (1)$$

where the k 's are rate constants for the anodic and cathodic processes respectively, $f_{M^{+n}}$ the activity coefficient of ion M^{+n} , $(C_{M^{+n}})_x = 0$ the concentration of ion M^{+n} at the electrode surface, and A the area of the electrode. Equation (1) is written on the assumption that the activity of the metallic electrode is unity and that the anodic process is controlled by a single rate determining step. Furthermore it will be assumed that A is constant during electrolysis, i.e. that there is no preferential attack.

The current can also be written in terms of the flux of ion M^{+n} at the electrode surface. Thus

$$i = -nFA D_{M^{+n}} \left(\frac{\partial C_{M^{+n}}}{\partial x} \right)_{x=0} \quad (2)$$

where $D_{M^{+n}}$ is the diffusion coefficient of ion M^{+n} . The calculation of the derivative in (2) is exceedingly difficult in the case of a stirred solution even under the case of laminar flow⁶, and an approximate solution based on

(6) See for example B. Levich, Acta Physicochim. U. R. S. S., 17, 257 (1942).

Nernst's concept of diffusion layer will be given here. Thus

$$\left(\frac{\partial C_{M^{+n}}}{\partial x} \right)_{x=0} = - \frac{(C_{M^{+n}})_{x=0} - C_{M^{+n}}^0}{\delta} \quad (3)$$

where $C_{M^{+n}}^0$ is the concentration of ion M^{+n} in the bulk of solution, and δ the thickness of the diffusion layer. Since δ is very small in comparison with the dimensions of the vessel, $C_{M^{+n}}^0$ at time t is

$$C_{M^{+n}}^0 = \frac{\int_0^t i dt}{n F V} \quad (4)$$

where V is the volume of solution.

By combining equations (1) to (4) one obtains a differential equation whose solution is

$$i = nFAk_a \exp \left[- \frac{AD}{V\delta \left(\frac{D}{k_c\delta} + 1 \right)} t \right] \quad (5)$$

This solution is written for $C_{M+n}^* = 0$ at $t = 0$. The average rate of oxidation W for a duration τ is obtained from (5) by application of Faraday's law. If one assumes that δ is independent of time, one obtains

$$W = W_M k_a \frac{1 - \exp(-\lambda\tau)}{\lambda\tau} \quad (6)$$

where W_M is the atomic weight of metal M and λ is defined by

$$\lambda = \frac{AD}{V\delta \left(\frac{D}{k_c\delta} + 1 \right)} \quad (7)$$

The function of the dimensionless group $\lambda\tau$ in equation (7) is equal to unity for $\lambda\tau = 1$; this function, which decreases as $\lambda\tau$ increases, approaches zero for sufficiently large values of $\lambda\tau$. Two important conclusions can be drawn from equation (7).

(1) When the potential is sufficiently anodic, k_c and consequently λ , is very small; equation (7) can then be written under the form $W = W_M k_a$. Since k_a is an exponential function of the electrode potential, a plot of $\log W$ versus potential should yield a straight line. This is essentially the case in Fig. 2 for potentials more anodic than -0.2 volt. As the potential is made more anodic the influence of the cathodic process becomes more pronounced, i.e.

k_a increases. The rate W is thus smaller than one would expect from proportionality between W and $W_M k_a$, and there is a departure from linearity in the diagram of Fig. 3. No precise calculation of the dependence of k_a on potential can be deduced from Fig. 2 because of the following cause of errors: the value of the potential of the working electrode with the cell of Fig. 1 includes the ohmic drop between the end of canal C and the surface of the electrode. It would be difficult to evaluate this error, although it could be minimized by decreasing the diameter of canal C. However, this solution is not practical because the canal C is then too easily plugged when a precipitate (see below) is formed at the surface of the working electrode.

(2) The average value of W at a given potential depends on the duration of electrolysis. Thus, λ is constant at a given potential, but $\lambda \tau$ obviously increases with the duration of electrolysis, and the function of $\lambda \tau$ in (6) decreases. This effect is apparent from the data of Fig. 4. There is some discrepancy between theory (curve) and experiment for the longer durations of electrolysis. This may result from variations in the electrode area while it was assumed in the above analysis that this area is constant. In quoting rates of anodic oxidation at constant potential it is therefore essential to indicate the duration of electrolysis. It might seem preferable to report values of k_a and λ , but these data could be used only for cases in which the above treatment is applicable; this would not be so when films are formed (see below) or when the anodic process cannot be accounted for by equation (1).

OXIDATION IN ACETATE BUFFER.

Results for acetate buffers of different pH's are summarized in Fig. 5.

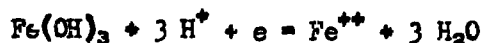
These results can be conveniently discussed by considering the potential-pH diagram of iron as established by Pourbaix⁸. It should be emphasized that

(8) M. Pourbaix, "Thermodynamique des Solutions Aqueuses Diluées" -
Représentation Graphique du Rôle du pH et du Potentiel" (Thesis) Delf, Meinema,
1945. English translation by J. M. Agar, Arnold, London, 1949.

this diagram supplies only equilibrium conditions⁹, while experimental results obviously depend on the kinetics of the reactions being considered.

(9) The construction of potential-pH diagrams is based on a systematic application of the Nernst equation.

The use of the potential-pH diagram is nevertheless fruitful in the elucidation of experimental results. Inspection of the diagram for iron shows that between pH 4 and 6 the oxidation of iron proceeds with the formation of Fe⁺⁺ ions. The equilibrium between Fe⁺⁺ ions and Fe(OH)₃



must also be considered. The corresponding equilibrium potential at 25° is ¹⁰

(10) P. Delahay, M. Pourbaix, P. Van Rysselberghe, J. Chem. Education, 27, 683 (1950).

$$E = 1.044 - 0.177 \text{ pH} - 0.0591 \log a_{\text{Fe}^{++}} \quad (8)$$

The standard potential in equation (8) varies somewhat according to the standard free energy one adopts for $\text{Fe}(\text{OH})_3$, i.e. according to the solubility product of this substance. Latimer's value¹¹ of -166.0 kcal.

(11) W. M. Latimer, "The Oxidation States of the Elements and their Potentials in Aqueous Solutions", 2nd. Ed., ^WPrentice-Hall, New York, N. Y., 1952, p. 221.

was used here.

One calculates from (8) that $E = 0.327$ volt for $\text{pH} = 4.05$ and $a_{\text{Fe}^{++}} = 1$. There is therefore a relatively large equilibrium concentration of ferrous ion up to potentials as anodic^{as}, say, 0.3 - 0.4 volt. At more anodic potentials ferric hydroxide is formed and the curve for $\text{pH} 4.05$ in Fig. 5 levels off progressively. At $\text{pH} 4.99$ and 5.37 the behavior of iron is somewhat different from that at $\text{pH} 4.05$; there is rapid drop in the rate of oxidation between 0.1 and 0.3 volt. This probably results from the formation of ferric hydroxide at the electrode surface. At 0.3 volt, one has approximately $a_{\text{Fe}^{++}} = 10^{-3}$, but this value is quite uncertain because the ΔF° for $\text{Fe}(\text{OH})_3$ used in the calculation corresponds to a solubility product of 6×10^{-38} for ferric hydroxide. Values as low as 10^{-42} have been reported for this datum⁸ and the resulting value of $a_{\text{Fe}^{++}}$ at $\text{pH} 5.37$ and 0.3 would be much lower than 10^{-3} (10^{-6} or so). In

conclusion, the formation of $\text{Fe}(\text{OH})_3$ probably causes the rapid drop in the rate of oxidation at pH 4.99 and 5.37. This effect is far less pronounced at pH 4.05.

The more or less linear segments between -0.7 and 0 volt in Fig. 4 should be shifted to more cathodic potentials by 0.177 volt per increase of one pH unit (see equation (8)). Actually there is a shift in the right direction, but the relative lack of precision of experimental data does not allow one to reach any further conclusion.

Because of the complexity of anodic processes which yield insoluble substances no attempt was made to develop a quantitative treatment.

OXIDATION IN BORATE BUFFER.

Data for the oxidation in borate buffer of pH 9.0 are listed in Table I. There was virtually no oxidation at potentials less anodic than 1.0 volt. Pitting of the electrode was observed at more anodic potentials. This observation can be explained as follows. Oxygen is evolved at these very anodic potentials. Since the surface of the electrode is not uniform, oxygen evolution occurs in these areas of the electrode surface where the overvoltage for this reaction is lower than in the other parts of the electrode. The evolution of oxygen is accompanied by the liberation of hydrogen ion and by a local decrease in the pH of the solution. The solubility of ferric hydroxide is increased accordingly in these areas where the oxygen is evolved, and there is a high rate of localized oxidation.

OXIDATION IN SODIUM HYDROXIDE.

Rates of anodic oxidation in 0.1 N. sodium hydroxide were too low to be

measurable with precision. No experiment was made above pH 13 because of the danger of attack of the circulating pump (rubber part).

ACKNOWLEDGMENT.

The support of this investigation by the Office of Naval Research is gladly acknowledged. The authors are indebted to Messrs. W. Payne and T. Leinhardt for their help in the construction of the potentiostat.

TABLE I

ANODIC OXIDATION OF IRON IN BORATE BUFFER OF pH 9.0

Potential Volts <u>vs.</u> N.H.E.	Rate of Oxidation $\text{mg.cm.}^{-2}\text{hr}^{-1}$
-0.757	0.1
+1.098	0.1
+1.250	0.17
+1.444	0.45
+1.549	3.70
+1.706	7.19

(1) Smaller than experimental errors

LIST OF FIGURES

Fig. 1. Schematic diagram of potentiostat. T_1 , isolation transformer, 350 watts; T_2 , isolation transformer, 150 watts; T_3 and T_4 , "Powerstat" transformer, 3 amp. output; R_1 , selenium bridge rectifier, 114 volts, 0.9 amp.; R_2 , selenium bridge rectifier, 168 volts, 2.4 amp.; C_1 to C_4 , electrolytic condenser, 125 microfarads, 350 volts; C_5 to C_8 , electrolytic condenser, 250 microfarads, 350 volts; r_1 to r_3 , ²⁵ohms, 50 watts; r_4 , 40 ohms, 200 watts; r_5 to r_7 , 10 ohms, 200 watts; r_8 to r_{10} , shunts for meter A to give readings of 0.05, 0.5, and 5 amp., respectively; r_{11} , 20 K., 20 watts; r_{12} , 10 K., 20 watts; r_{13} , 5 K., 20 watts; r_{14} , 2 K., 20 watts; r_{15} , 1K., 20 watts; r_{16} , 500 ohms, 50 watts; r_{17} , 200 ohms, 100 watts; r_{18} , 100 ohms, 100 watts; r_{19} , 50 ohms, 100 watts; r_{20} , 25 ohms, 200 watts; p_1 , potentiometer, 16 ohms, 100 watts; p_2 , "Helipot" potentiometer, 1000 ohms, 10 turns, 0.1%; p_3 , potentiometer, 2000 ohms, wire-wound; p_4 , potentiometer, 200 ohms, wire-wound; S_5 , D.P.D.T. switch; S_7 and S_8 limit switches; S_9 push-button switch; b_1 , 6 volt storage battery; Br, "Brown" amplifier model #356358-1; M, "Brown" reversible motor, model #76750-3; V_1 , 0-150 volt, voltmeter; V_2 , 0-3 volt, voltmeter; A, 0-5 milliamp. ammeter.

Fig. 2. Electrolytic cell and accessories.

Fig. 3. Variations of the rate of anodic oxidation of iron (in 0.1 N perchloric acid with potential. Duration of electrolysis, 2 hours.

Fig. 4. Variations of the rate of anodic oxidation of iron with duration of electrolysis. Points are experimental values; curve calculated for $\lambda = 0.0533 \text{ min.}^{-1}$

Fig. 5. Variations of the rate of oxidation of iron in acetate buffers with potential. Duration of electrolysis, 2 hours.

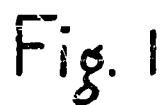


Fig. 1

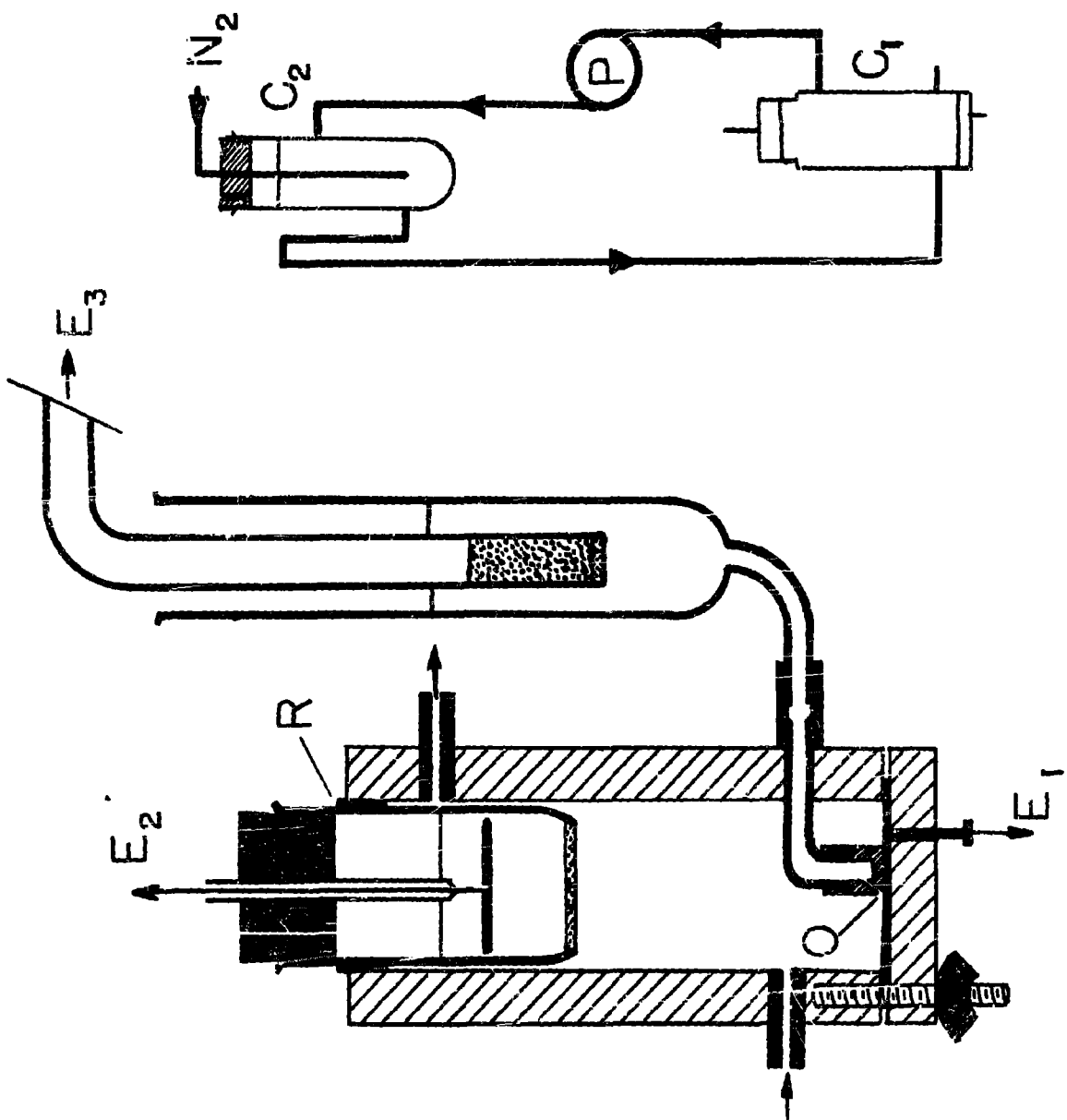


FIG. 2

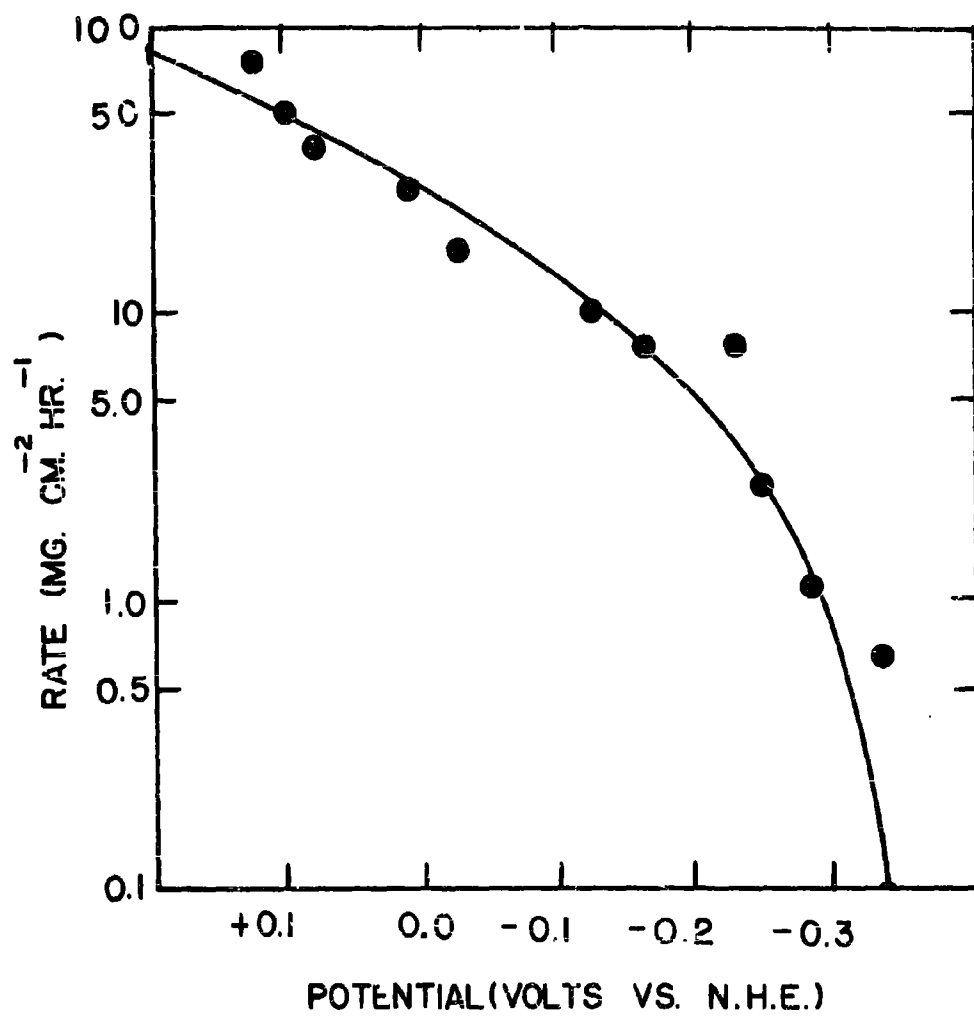


FIG. 3

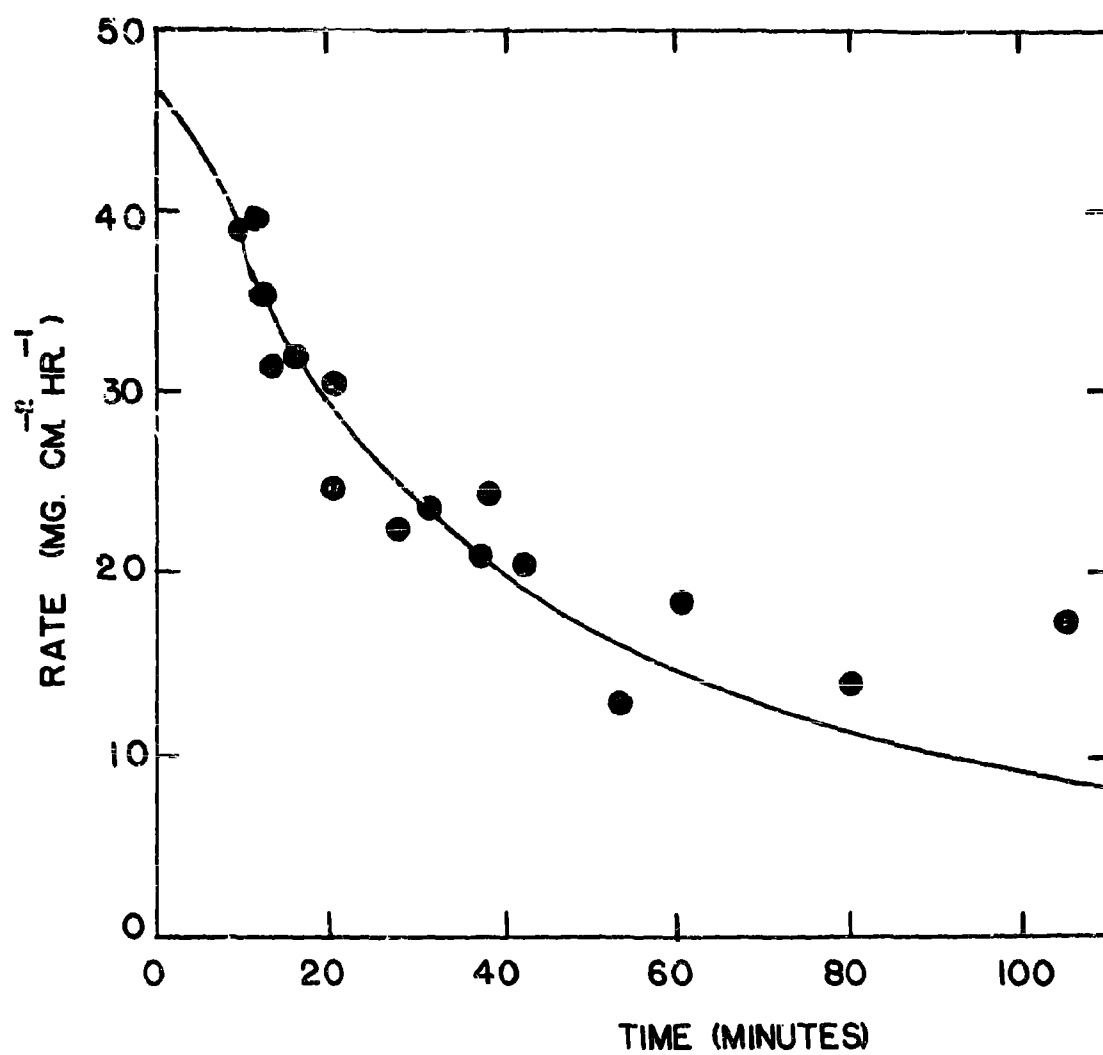


FIG. 4

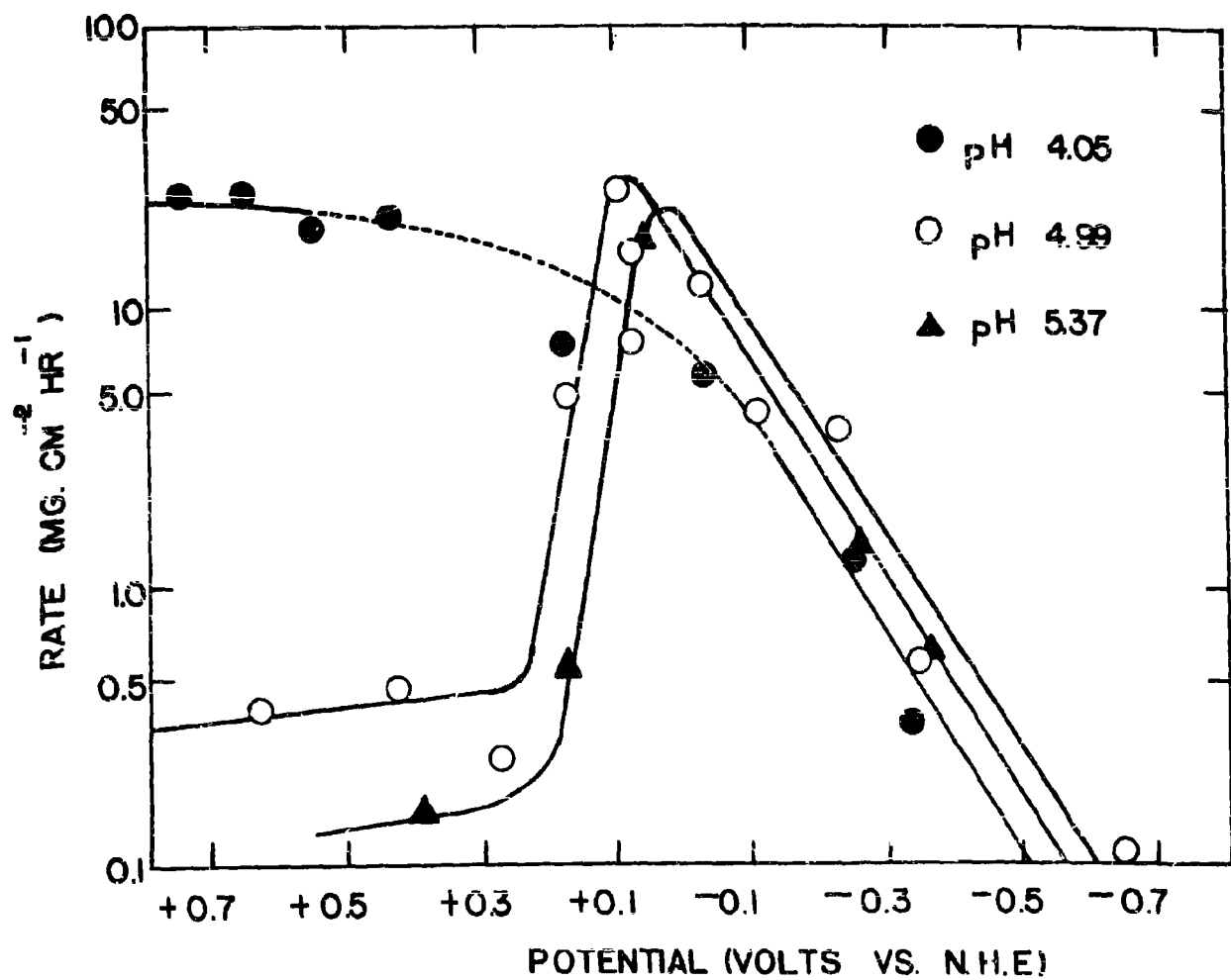


FIG. 5

Armed Services Technical Information Agency

AD

32269

NOTICE: WHEN GOVERNMENT OR OTHER DRAWINGS, SPECIFICATIONS OR OTHER DATA ARE USED FOR ANY PURPOSE OTHER THAN IN CONNECTION WITH A DEFINITELY RELATED GOVERNMENT PROCUREMENT OPERATION, THE U. S. GOVERNMENT THEREBY INCURS NO RESPONSIBILITY, NOR ANY OBLIGATION WHATSOEVER; AND THE FACT THAT THE GOVERNMENT MAY HAVE FORMULATED, FURNISHED, OR IN ANY WAY SUPPLIED THE SAID DRAWINGS, SPECIFICATIONS, OR OTHER DATA IS NOT TO BE REGARDED BY IMPLICATION OR OTHERWISE AS IN ANY MANNER LICENSING THE HOLDER OR ANY OTHER PERSON OR CORPORATION, OR CONVEYING ANY RIGHTS OR PERMISSION TO MANUFACTURE, USE OR SELL ANY PATENTED INVENTION THAT MAY IN ANY WAY BE RELATED THERETO.

Reproduced by
DOCUMENT SERVICE CENTER
KNOTT BUILDING, DAYTON, 2, OHIO

UNCLASSIFIED